Available online at www.sciencedirect.com
ScienceDirect
Journal of Nuclear Materials 367–370 (2007) 107–111
journal of nuclear materials
www.elsevier.com/locate/jnucmat

Effects of heat treatment and irradiation on mechanical properties in F82H steel doped with boron and nitrogen

N. Okubo *, E. Wakai, S. Matsukawa, T. Sawai, S. Kitazawa, S. Jitsukawa

Japan Atomic Energy Agency, Shirakata 2-4, Tokai-mura, Ibaraki-ken 319-1195, Japan

Abstract

Effects of heat treatment and irradiation on mechanical properties and microstructures have been studied for martensitic steel F82H co-doped with 60 ppm B and 200 ppm N (F82H + B + N) to evaluate fundamental mechanical properties and irradiation response before irradiation at JMTR and HFIR facilities. The specimens were firstly normalized at 1150 °C and tempered at 700 °C, secondly normalized at 1000 °C and tempered at 700, 750 and 780 °C. The tensile properties were measured for the specimens before irradiation. Single ion irradiations of 10.5 MeV Fe^{3+} and dual ion irradiations of 10.5 MeV Fe^{3+} with simultaneous 1.05 MeV He^{+} of 10 appmHe/dpa rate were performed at 160–590 °C to 20 dpa. Micro-hardness was measured before and after the irradiation. Tensile properties of the F82H + B + N were similar to F82H and also radiation hardening behaved similarly to F82H. The change of hardening increased with increasing temperature, saturated around 350 °C and decreased at higher temperature.

1. Introduction

Reduced activation ferritic/martensitic steels are primary candidate materials for nuclear fusion reactors [1–3]. The fast neutrons cause displacement damage and produce transmutation products such as helium (He) atoms in the materials. It is necessary to understand the effects of the simultaneous formation of displacement damage and large amounts of He on mechanical properties and microstructures, and the dependence on irradiation temperature [4–8]. Boron (B) doping has been used in steels to modify toughness by B segregation and/or precipitation on prior austenitic grain boundaries [9]. The B doping of steels is also frequently conducted to simulate effects of He production on microstructural evaluation in fusion reactors by utilizing the $^{10}B(n, \alpha)^{7}Li$ reaction in a mixed spectrum of thermal and fast neutrons in a fission reactor [10]. The B doping in steels, however, may cause the ductility loss, and mask the real effects of the irradiation. In a previous study, B doping of the martensitic steel F82H caused irradiation hardening [11], but the B doping degraded the original fracture toughness of the F82H [12]. The mechanical properties of F82H doped with B before irradiation should be almost equal with those of undoped F82H to evaluate He effects accurately. We used co-doped material to

* Corresponding author. Tel.: +81 29 282 6563; fax: +81 29 282 5922.
E-mail address: okubo.nariaki@jaea.go.jp (N. Okubo).

0022-3115/$ - see front matter © 2007 Elsevier B.V. All rights reserved.
doi:10.1016/j.jnucmat.2007.03.159

modify the mechanical properties of B containing specimens. In previous studies, co-doping of B and nitrogen (N) in F82H steels (F82H + B + N) suppressed B localization, and an appropriate heat treatment improved the mechanical properties of the F82H co-doped with B and N [12,13]. In order to evaluate the effects of He produced during irradiation on the mechanical properties of F82H, the F82H + B + N will be used in spectrally tailored irradiations in the high flux isotope reactor (HFIR), experiment HFIR-15J. Irradiation in the Japan Materials Testing Reactor (JMTR) is also proposed to evaluate preirradiation tempering effects on the mechanical properties of irradiated material. To further understand the fundamental mechanical properties and irradiation response of F82H + B + N steels, the effects of heat treatment on mechanical properties are examined. Some information on the hardening behavior due to ion irradiation is also presented.

2. Experimental procedures

Specimens used in this study were F82H (Fe–8Cr–2W–0.3V–0.04Ta–0.1C) martensitic steels, and F82H steels co-doped with 60 mass ppm B and 200 ppm N, typically shown as F82H + B + N. The undoped F82H steel was used for comparison specimen. The isotope of ^{10}B and ^{11}B was separately doped in F82H steels co-doped with N; these materials were denoted F82H + 10B + N and F82H + 11B + N, respectively. Chemical compositions of the specimens are given in Table 1. The F82H (IEA-heat) steels were normalized at 1040 °C for 2.2 ks followed by air cooling (AC) and tempered at 750 °C for 3.6 ks followed by AC, which was termed a single heat treatment. The F82H + B + N and F82H (except IEA-heat) steels were firstly normalized at 1150 °C for 1.8 ks followed by water quench (WQ) and tempered at 700 °C for 7.2 ks followed by air cooling (AC), and subsequently normalized at 1000 °C for 0.6 ks followed by WQ and tempered at various temperatures of 700 °C for 3.6 ks, 750 °C for 3.6 ks or 780 °C for 1.8 ks followed by AC, which was termed a dual heat treatment. Tensile tests were performed at room temperature in air and at 250 and 350 °C in vacuum, with loading rate of 3.3×10^{-6} m/s. Sheet tensile specimens were 25.4 mm long and 0.76 mm thick, the gage length and width are 7.62 and 1.52 mm, respectively. Ductile–brittle transition temperatures (DBTT) were measured by Charpy V notched impact test, with specimen size 20 mm long, 3.0 mm wide and 1.5 mm thick. The notch depth was 0.5 mm.

Ion irradiations at the TIARA facility in JAEA were performed with 10.5 MeV-Fe^{3+} (single irradiation) and 10.5 MeV-Fe^{3+} with simultaneous 1.05 MeV-He^{+} ions (dual irradiation) to 20 dpa at several temperature in the range of 160–590 °C. Hardening behavior of the irradiated F82H + 10B + N steel was evaluated using a nano indentator, with maximum loading force set to 10 mN. The micro-hardness was calculated from mean values of 30 points per specimen. The microstructures and the precipitate sizes of the specimens were evaluated using a transmission electron microscope (TEM) operated at 200 kV.

3. Results and discussion

Tensile properties of F82H + 10B + N and F82H + 11B + N steels are nearly equivalent. Yield stress (YS), ultimate tensile stress (UTS) and total elongation (TE) of F82H + 10B + N and F82H + 11B + N steels tempered at 700, 750 and 780 °C with the dual heat treatment are shown in Table 2 for room-temperature measurements. The YS and UTS of the F82H + 10B + N steel decreased with increasing normalizing temperature. The YS of the F82H + 10B + N steel tempered at 700, 750 and 780 °C was 710, 580 and 500 MPa, respectively. The YS and UTS of the F82H + 10B + N steel are similar to that of the F82H + 11B + N steel as shown in Table 2 and also to that of the undoped F82H. The TE of the F82H + 10B + N increases with increasing tempering temperature and is similar to that of the F82H + 11B + N. In the measurements at 250 and 350 °C, the YS of F82H + 10B + N tempered at 780 °C decreased to 450 and

Table 1
Chemical compositions of the F82H steels (mass %)

	B	N	Cr	W	C	O	Al	Si	P	S	Ti	V	Mn	Ta
F82H	–	–	8.10	2.02	0.10	0.0055	0.001	0.10	0.005	0.001	0.002	0.31	0.13	0.034
F82H + B + N	0.0059	0.019	8.09	2.10	0.10	0.0041	<0.001	0.10	0.006	0.001	0.002	0.30	0.10	0.039

Table 2
Tensile and DBTT data of F82H, F82H + 10B + N and F82H + 11B + N tempered at 700–780 °C with dual heat treatment

	Tempering temperature (°C)	YS (MPa)	UTS (MPa)	UE (%)	TE (%)	DBTT (°C)
F82H	750	569	663	5.5	16.6	−50
F82H + 10B + N	700	712	807	4.3	12.3	−55
F82H + 10B + N	750	578	702	5.3	13.4	−85
F82H + 10B + N	780	502	642	7.9	19.8	−85
F82H + 11B + N	700	735	837	4.3	12.6	–
F82H + 11B + N	750	528	662	6.2	15.6	–
F82H + 11B + N	780	502	645	7.4	18.8	–

430 MPa, respectively. The dependence of YS on tempering temperature could be qualitatively explained by microstructural evaluations as mentioned later.

The effect of tempering temperature on DBTT of F82H + 10B + N steels was evaluated. The DBTT of the specimens tempered at 700, 750 and 780 °C was about −55, −85 and −85 °C, respectively, as shown in Table 2. Upper shelf energy was not dependent on the tempering temperature and nearly constant in the tempering temperature region of 700–780 °C. The DBTT of the specimen tempered at 700 °C was about 30 °C higher than those of the specimens tempered at 750 and 780 °C. The specimens tempered at 750 and 780 °C had better fracture toughness than the specimens tempered at 700 °C, which absorbed energy was almost zero *J* below −100 °C. Correlations between tempering temperature, YS and DBTT in the F82H + 10B + N steels were evaluated. The DBTTs of the specimens tempered at 700 and 750 °C correspond to the YS dependence on the tempering temperature. The DBTT of the specimens tempered at 780 °C, however, is comparable to that of specimens tempered at 750 °C. The DBTT of the specimens tempered at 780 °C does not decrease and does not depend on the YS.

Typical TEM images of F82H + 10B + N steels tempered at 700, 750 and 780 °C are shown in Fig. 1(1)–(3), respectively. Lath boundaries about 400–500 nm wide and precipitates observed as black contrasts and dislocation lines were similarly seen in all specimens. The precipitations were identified as carbides by using electron diffraction. The mean size of the precipitations was about 110 nm for the specimen normalized at 700 °C. The mean sizes of the precipitations in the specimens normalized at 750 and 780 °C were similar, with size about 130 nm. The mean precipitate size in the F82H + 10B + N was slightly larger than that of undoped F82H as when compared at the same tempering temperature.

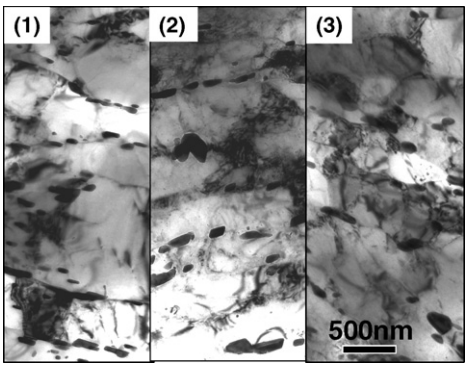

Fig. 1. Microstructures of F82H + B + N steels tempered at various temperatures. Tempering was performed at (1) 700; (2) 750 and (3) 780 °C. The size of precipitates slightly increases with tempering temperature, with values of 130 nm (1), 145 nm (2) and 160 nm (3).

The number density of precipitations tempered at 700, 750 and 780 °C was 2.0×10^{20}, 1.3×10^{20} and 1.4×10^{20} m^{-3}, respectively. The mean number density of precipitations in the specimen tempered at 780 °C increased slightly compared with the specimen tempered at 750 °C. The density of dislocations in material tempered at 700, 750 and 780 °C was 1.1×10^{14}, 6.1×10^{13} and 2.5×10^{13} m^{-2}, respectively. The dislocation density decreased with increasing tempering temperature, and caused the reduction of tensile strength shown in Table 2. Changes in DBTT correlate with changes in mean size and number density of precipitates, not with changes in dislocation density, for the specimen tempered at 780 °C. The YS of F82H + 10B + N was similar to that of nondoped F82H, but the density of dislocations of F82H + 10B + N (6.1×10^{13} m^{-2}) was smaller than that of undoped F82H (2×10^{14} m^{-2}[14]) at the same tempering temperature of 750 °C. The results suggest that the change in DBTT of F82H + 10B + N depends on the tempering temperature, and is related to both the dislocations and precipitates, which may act as obstacles to dislocation movement.

Changes in the micro-hardness of the F82H + 10B + N and F82H (IEA-heat) steels due to irradiation to dose of 20 dpa are shown in Fig. 2. These specimens were tempered at 780 °C. Normalized hardness (micro-hardness after irradiation divided by that before irradiation) of both steels showed a similar dependence on dpa. The hardness increased with increasing dpa and tended to saturate at about 1.5 times the unirradiated value. Comparing the single and dual irradiations, differences were not observed at this dpa level. It is noted that the same behavior of radiation hardening in the F82H + 10B + N and F82H is essential for estimating He effects and this results is helpful for validation of the doping method.

A typical cross sectional TEM image of F82H + B + N steel irradiated by single Fe ion to 10 dpa is shown in Fig. 3. Bright field (BF) image and weak beam dark field (WBDF) image at about 1 μm depth are also shown in the figure. The microstructures of the irradiated specimen consisted of interstitial-type loops, with mean size about 20 nm, and smaller defect clusters and a high density of dislocation lines. Comparing with non-irradiated specimens, these loops and defect clusters contribute to the radiation hardening, but further microstructural evaluation is necessary for more detailed comparisons.

The temperature dependence of radiation hardening was similar for F82H + B + N and F82H steels. Micro-hardness before/after irradiation at several temperatures and the temperature dependence of radiation hardening are shown in Fig. 4. The hardening ratio increases from 1.1 to 1.4 as

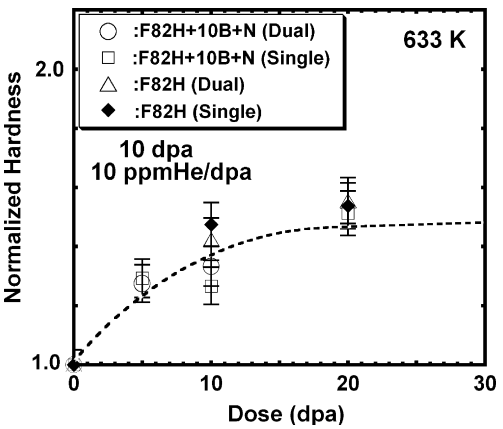

Fig. 2. Dose dependence of radiation hardening for irradiated F82H + 10B + N steels. Specimens were irradiated at 360 °C by 10.5 MeV Fe^{3+} and by simultaneous 1.05 MeV-He^{+} ions.

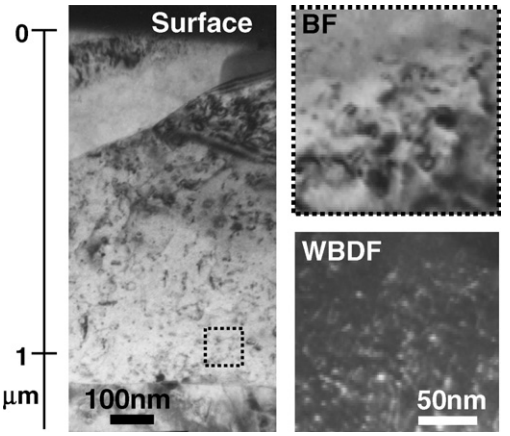

Fig. 3. Cross sectional TEM images of F82H + B + N steel irradiated by single Fe ion to 10 dpa The specimen was tempered at 780 °C. The mean size of dislocation loop was about 20 nm.

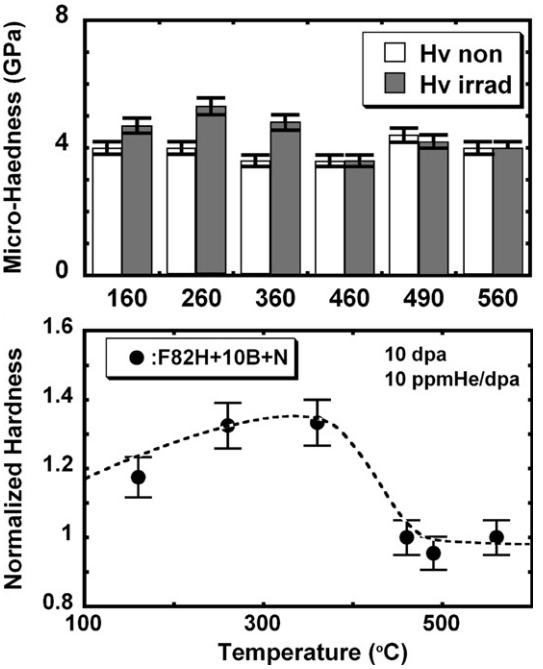

Fig. 4. Micro-hardness before/after irradiation at several temperatures and temperature dependence of the radiation hardening.

temperature increases from 160 to 360 °C and saturates around 350 °C. For higher irradiation temperatures, above 350 °C, the hardening decreased and is less important than the swelling caused at the higher temperatures. Compared with the case of F82H steels [15], though there was some scatter of the data. The F82H + 10B + N steels had the same

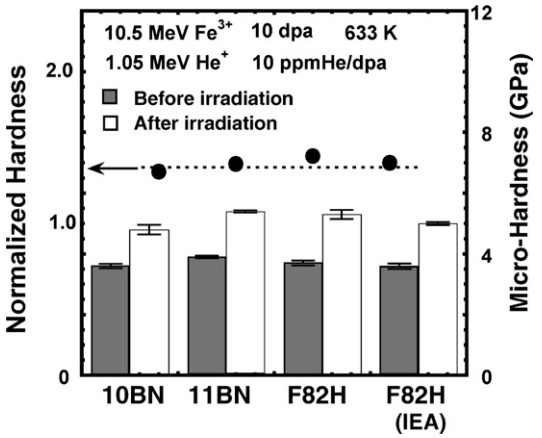

Fig. 5. Micro-hardness before/after irradiation and radiation hardening of F82H + 10B + N, F82H + 11B + N, F82H and F82H IEA-heat.

radiation dependence on irradiation temperature as the F82H steel.

Micro-hardness before and after irradiation and radiation hardening of F82H + 10B + N, F82H + 11B + N, F82H and F82H IEA-heat are shown in Fig. 5. All of the steels had the same hardening ratio of about 1.4 for displacement damage of 10 dpa. Distinct differences in radiation hardening were not observed between F82H + 10B + N, F82H + 11B + N and undoped F82H steels. It is noted that the same level of radiation hardening in these steels shows suppression effect of B doping in F82H on mechanical properties and radiation hardening when co-doping of B and N is used.

4. Conclusion

Effects of tempering treatment on mechanical properties and microstructures have been studied for the ferritic/martensitic steel F82H doped with 60 ppm B (^{10}B and ^{11}B) and 200 ppm N. Tensile strength, for which no difference was observed between F82H + 10B + N and F82H + 11B + N, depended on tempering temperature and corresponded to the density of dislocations. Hardening of F82H + B + N after irradiation at several temperatures was found to be comparable with that of undoped F82H. Hardening behavior due to ion irradiation of the F82H + B + N was comparable to that for the F82H. The unfortunate increment of radiation hardening, which was caused by doping steels only with B, was not observed in the dual doped F82H + 10B + N. The mechanical properties and irradiation response of F82H co-doped with B and N shows that the material is suitable for accurate simulation of He effects for irradiation in JMTR and HFIR.

References

[1] A. Kohyama, M. Seki, K. Abe, T. Muroga, H. Matsui, S. Jitsukawa, S. Matsuda, J. Nucl. Mater. 283–287 (2000) 20.
[2] R.L. Klueh, D.S. Gelles, S. Jitsukawa, A. Kimura, G.R. Odette, B. van der Schaaf, M. Victoria, J. Nucl. Mater. 307–311 (2002) 455.
[3] A. Hishinuma, A. Kohyama, R.L. Klueh, D.S. Gelles, W. Dietz, K. Ehrlich, J. Nucl. Mater. 258–263 (1998) 193.
[4] A. Kimura, R. Kasada, R. Sugano, A. Hasegawa, H. Matsui, J. Nucl. Mater. 283–287 (2000) 827.
[5] R.L. Klueh, M.A. Sokolov, K. Shiba, Y. Miwa, J.P. Robertson, J. Nucl. Mater. 283–287 (2000) 478.
[6] D.S. Gelles, J. Nucl. Mater. 283–287 (2000) 838.
[7] M. Rieth, B. Dafferner, H.-D. Röhrig, J. Nucl. Mater. 258–263 (1998) 1147.
[8] P. Jung, H. Henry, J. Chen, J.-C. Brachet, J. Nucl. Mater. 318 (2003) 241.
[9] M. Ueno, K. Ito, Irons Steels 74 (1988) 910.
[10] N. Hashimoto, R.L. Klueh, K. Shiba, J. Nucl. Mater. 307–311 (2002) 222.
[11] E. Wakai, S. Matsukawa, T. Yamamoto, Y. Kato, F. Takada, M. Sugimoto, S. Jitsukawa, Mater. Trans. 45 (8) (2004) 2642.
[12] E. Wakai, M. Sato, T. Sawai, K. Shiba, S. Jitsukawa, Mater. Trans. 45 (2) (2004) 407.
[13] N. Okubo, E. Wakai, S. Matsukawa, K. Furuya, H. Tanigawa, S. Jitsukawa, Mater. Trans. 46 (2) (2005) 194.
[14] E. Wakai, N. Hashimoto, Y. Miwa, J.P. Robertson, R.L. Klueh, K. Shiba, S. Jitsukawa, T. Yamamoto, F. Takada, J. Nucl. Mater. 283–287 (2000) 799.
[15] M. Ando, E. Wakai, T. Sawai, H. Tanigawa, K. Furuya, S. Jitsukawa, H. Takeuchi, K. Oka, S. Ohnuki, A. Kohyama, J. Nucl. Mater. 329–333 (2004) 1137.